Available online at www.sciencedirect.com
ScienceDirect
Neurocomputing 70 (2006) 200–205
NEUROCOMPUTING
www.elsevier.com/locate/neucom

Inhibitory control of spike timing precision ☆

M. Ambard*, D. Martinez

CORTEX Group, LORIA-INRIA, Nancy, France

Received 5 August 2005; received in revised form 24 February 2006; accepted 24 March 2006
Communicated by Lansner
Available online 7 July 2006

Abstract

GABAergic inhibition via local interneurons may play a role in enhancing spike timing precision in principal cells, since it tends to eliminate the influence of initial conditions. However, both the number and the timing of inhibitory synaptic events may be variable across repeated trials. How does this variability affect the spike timing precision in principal neurons? In this paper, we derive an analytical expression for the spike output jitter as a function of the variability of the received inhibition. This study predicts that variable inhibition is especially tolerated as the number of inhibitory cells is large and the decay time constant of the GABAergic synapse is small, which is consistent with experimental data from early olfactory systems (antennal lobe for insects, olfactory bulb for vertebrates).

Keywords: Firing precision; GABAergic inhibition; Spiking neurons; Olfaction; Olfactory bulb

1. Introduction

Experimental evidence tends to show that precise spike timing plays a significant role in the encoding of sensory stimuli [23]. A pre-requisite is that neurons fire spikes in a precise and reproducible way over repeated presentations of the same stimulus. Both experimental studies and theoretical work have shown that the neural response can indeed be precise and reliable, depending on the nature of the input [13,3,8]. Fast varying aperiodic stimuli lead to precise spike timing while constant or slowly varying stimuli yield imprecise firing. All natural stimuli, however, do not have a high-temporal bandwidth. For example, in comparison with sounds or images, odors change more slowly.

Olfaction is generally a slow-temporal bandwidth sense. Olfactory receptor neurons converge onto glomeruli that present a slow dynamics of activation [18]. Thus, olfactory bulb mitral cells (MCs), excited by one or few glomeruli, receive slowly varying inputs. It is known that MCs have an unreliable spiking activity under constant stimulation [1]. Despite this fact, some MCs present in vivo synchronization with precise spiking activity [9,7]. In the olfactory bulb, MCs receives inhibition from inhibitory granule cells (GCs). The received inhibition could be responsible of the precision of individual MCs, since it tends to eliminate the influence of initial conditions [2,10]. However, GABAergic inhibition released by the GCs and received by the MCs is asynchronous and variable across repeated trials [19,22]. How does the variability in the received inhibition affect the precision of principal cells? To address this question we shall use a quadratic integrate-and-fire neuron model that allows for analytic calculations. In Section 2, we describe our model and present simulations showing that GABAergic inhibition may enhance spike timing precision. In Section 3, we derive an approximate analytical expression for the spike output jitter as a function of the variability of the received inhibition. In Section 4, we demonstrate the validity of this approximation with simulation results. In Section 5, we discuss the predictions obtained from our study.

2. Model description and simulations

We consider here the quadratic integrate and fire (QIF) model which is known to be a very good approximation of

☆This work was funded by the European Network of Excellence GOSPEL (http://www.gospel-network.org).
*Corresponding author.
E-mail addresses: maxime.ambard@loria.fr (M. Ambard), dominique.martinez@loria.fr (D. Martinez).

0925-2312/$ - see front matter © 2006 Elsevier B.V. All rights reserved.
doi:10.1016/j.neucom.2006.03.010

any type 1 neuron [6]. The time evolution of the membrane potential V is described by the following equation

$$C\frac{dV}{dt} = q(V(t) - V_T)^2 + I - I_{th} - I_{GABA}(t) + I_{noise}(t) \quad (1)$$

in which I is a constant input current, I_{th} denotes the minimal current required for repetitive firing, I_{noise} is an intrinsic white noise current of standard deviation σ_{noise} and I_{GABA} is a synaptic inhibitory current. In the absence of any noise and synaptic current, the QIF neuron converges to the resting potential V_{rest} when $I = 0$ and fires as soon as V reaches the threshold V_{th}, when $I \geqslant I_{th}$. Right after the spike, V is reset to the value V_{reset}. The membrane capacitance C and resting potential V_{rest} have been derived from MC experimental data [12,16]. The other parameters have been fitted in order to obtain a similar frequency-current response as the MC conductance-based model in [20]. The parameters chosen for the QIF neuron are as follows: $C = 0.2\,\text{nF}$, $V_{rest} = -65\,\text{mV}$, $V_T = -60.68\,\text{mV}$, $q = 0.00643\,\text{ms V}^{-1}$, $I_{th} = 0.12\,\text{nA}$, $V_{th} = 30\,\text{mV}$ and $V_{reset} = -70\,\text{mV}$. The inhibitory synaptic current $I_{GABA}(t)$ in Eq. (1) results from the summation of GABAergic synaptic events originating from interactions with GCs. An unitary event, occurring at time t^f, is modeled by a simple exponential inhibitory post-synaptic current (IPSC). For $t \geqslant t^f$, we have

$$IPSC(t) = g\,e^{-(t-t^f)/\tau}(V(t) - E_{GABA}). \quad (2)$$

The maximum synaptic conductance is $g = 1\,\text{nS}$ [16], the synaptic time decay is $\tau = 6\,\text{ms}$ [14] and the reversal potential of the synapse is $E_{GABA} = -70\,\text{mV}$. Simulations were performed by integrating Eq. (1) with a fourth-order Runge–Kutta method with time step of 0.05 ms. Unless specified otherwise, the following random initialization was used. The initial membrane potential $V(t = 0)$ is taken randomly between V_{reset} and V_{th} such as the firing times obtained over repeated trials, from Eq. (1) with $I_{GABA} = 0$ and $I_{noise} = 0$, are uniformly distributed.

The QIF neuron is precise when its firing time T stays unchanged across repeated trials with the same input current I. A measure of precision is the spike time jitter σ_T which characterizes the temporal dispersion around cluster firing times induced by repeated trials (precise neuron = small σ_T). Fig. 1 shows the temporal evolution of σ_T, estimated over 100 repeated simulations of the QIF neuron (Eq. (1)), with $I_{GABA} = 0$ and different σ_{noise} values. The initial condition $V(t = 0)$ was similar in all trials. Due to I_{noise}, the spike time jitter σ_T increases over time so that the neuron becomes more and more imprecise. This is in agreement with previous works [13,3,8]. To see if the first spike can convey some information about the input, we performed repeated simulations for different I and random initial conditions. Fig. 2 shows the mean and standard deviation σ_T of the first spike latency for a QIF neuron, with and without GABAergic inhibition. When $I_{GABA} \neq 0$, 100 synchronous IPSCs are generated at time $t^f = 0$ according to Eq. (2). From Fig. 2, we see that σ_T is very large when $I_{GABA} = 0$ and very small when $I_{GABA} \neq 0$. GABAergic inhibition makes the neuron more precise so that its firing time T is a reliable estimate of I. Two examples of spike rasters are indicated in Fig. 2 for $I = 0.14\,\text{nA}$ and for $I_{GABA} = 0$ and $I_{GABA} \neq 0$. Could increased precision be obtained with excitation rather than

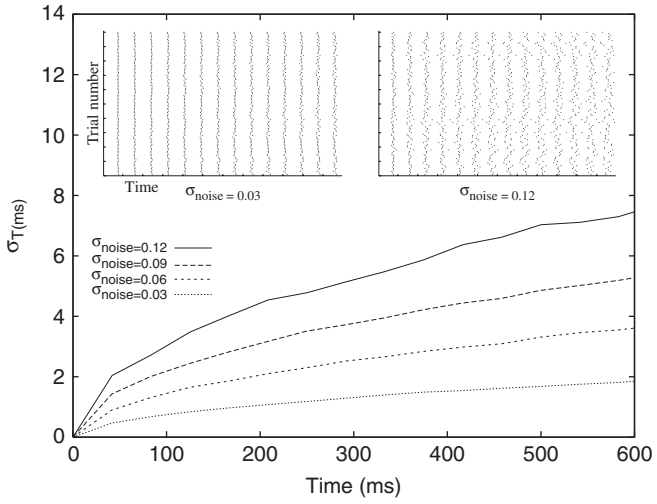

Fig. 1. Without GABAergic inhibition, the spike time jitter σ_T increases over time. The different curves indicate the temporal evolution of the spike time jitter σ_T estimated over 100 repeated simulations of the QIF neuron (Eq. (1)). In the simulations, $I = 0.15\,\text{nA}$, $I_{GABA} = 0$ and σ_{noise} ranges from 0.03 to 0.12 nA. Two examples of spike rasters obtained from 100 trials are indicated for $\sigma_{noise} = 0.03$ and 0.12 nA.

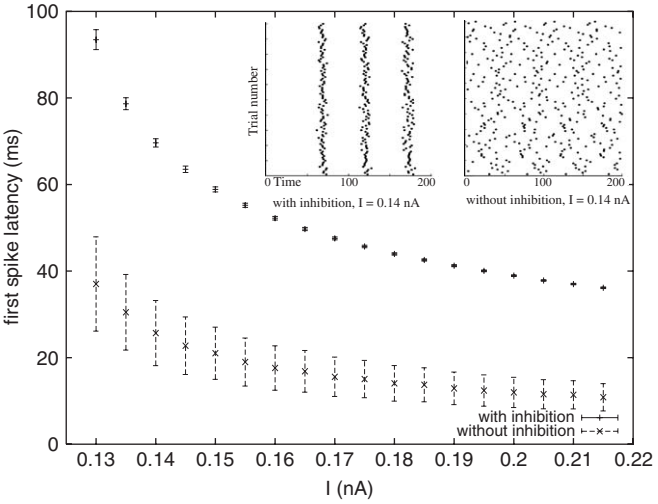

Fig. 2. Synchronous GABAergic inhibition enhances spike timing precision. Mean and standard deviation of the first spike latency as a function of the input current I have been estimated over 100 repeated simulations of the QIF neuron (Eq. (1), $\sigma_{noise} = 0.05\,\text{nA}$). The top curve is for $I_{GABA} \neq 0$ whereas the one at the bottom is for $I_{GABA} = 0$. $I_{GABA} \neq 0$ was obtained by the summation of 100 synchronous synaptic events occurring at time $t^f = 0$ and modeled by Eq. (2). Two spike rasters, obtained from repeated trials with $I = 0.14\,\text{nA}$, are indicated for $I_{GABA} = 0$ and $I_{GABA} \neq 0$.

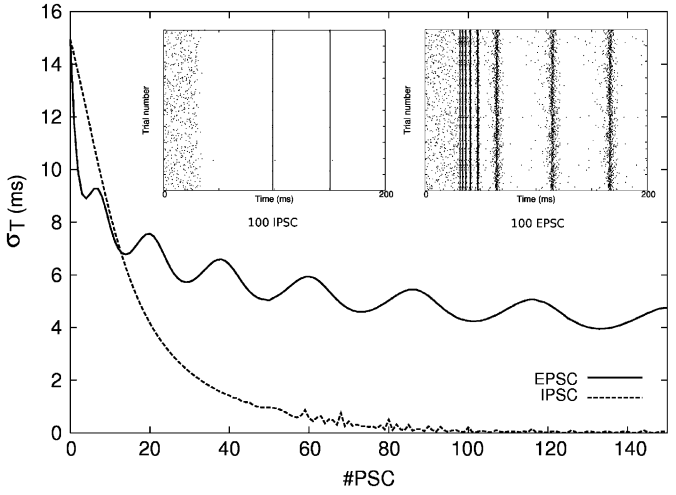

Fig. 3. Inhibitory versus excitatory control of spike timing precision. Plain and dashed curves represent the spike time jitter σ_T as a function of the number of received EPSCs and IPSCs, respectively. The spike time jitter was estimated after $t = 200$ ms on 1000 repeated simulations with $I = 0.14$ nA and random membrane potential initialization. Synaptic events were injected synchronously at $t = 30$ ms and their number varied in the simulations from 0 to 150. Two examples of spikes rasters are indicated for 100 IPSCs (left inset) and EPSCs (right inset).

inhibition? To address this question, we performed repeated simulations with a synaptic excitatory current I_{AMPA} replacing the GABAergic current in Eq. (1). I_{AMPA} results from the summation of unitary excitatory post-synaptic currents (EPSC) similar to Eq. (2) except that the reversal potential is now $E_{\mathrm{AMPA}} = 0$ mV [4]. EPSCs were injected synchronously at $t = 30$ ms; their number varied in the simulations from 0 to 150. The spike time jitter obtained is represented in Fig. 3 as a function of the number of received EPSCs, and compared to the one obtained with IPSCs under the same experimental conditions. This result shows that a high level of spike timing precision is not realized by excitation alone, even in presence of a large number of EPSCs. In contrast, GABAergic inhibition tends to eliminate the influence of initial conditions and, thus, leads to a high level of spike timing precision. This is in line with previous works [2,10]. In the olfactory bulb, the received inhibition from GCs could, therefore, be responsible for the precision of individual MCs. However, inhibitory feedback into the MCs is asynchronous and variable across trials [19,22]. How does the variability of the received inhibition affect the precision of principal neurons? This point will be studied mathematically in the next section.

3. Mathematical analysis of spike timing precision for a neuron receiving variable inhibition

Let us first consider a QIF neuron (Eq. (1) with $I_{\mathrm{noise}}(t) = 0$) receiving, at a time t^f, a single IPSC whose temporal evolution is given by Eq. (2). The total current, for $t \geqslant t^f$, is then

$$J(t) = I - I_{\mathrm{th}} - g\mathrm{e}^{-(t-t^f)/\tau}(V(t) - E_{\mathrm{GABA}}). \tag{3}$$

Börgers and Kopell [2] have shown that the firing time T_1 of a QIF neuron receiving a single strong IPSC is relatively independent of the initial condition $V(t = 0)$, see also [10]. Provided g is large enough, trajectories in the phase plane (V, J) are all attracted towards a given trajectory so that they all reach approximately the same point $(V_{\mathrm{th}}, J^\star)$ at firing time. This is shown in Fig. 3 in [10] and Fig. 5C in [2]. The result is an almost complete loss of the initial condition $V(t = 0)$. Whatever, the initial condition might be, the total input current is approximately equal to $J^\star$ at the firing time T_1

$$J^\star \approx J(T_1) = I - I_{\mathrm{th}} - g\mathrm{e}^{-(T_1-t^f)/\tau}(V_{\mathrm{th}} - E_{\mathrm{GABA}})$$

and thus

$$T_1 \approx \tau \ln g - \tau \ln(I - I_{\mathrm{th}} - J^\star) + \tau \ln(V_{\mathrm{th}} - E_{\mathrm{GABA}}) + t^f.$$

To determine the effect of variable inhibition on the spike time jitter, we have generalized Börgers and Kopell's study to the case of a QIF neuron receiving a burst of k IPSCs at times t_i^f, $i = 1, 2, \ldots, k$. Without loss of generality, we consider that the neuron fires after receiving the kth IPSC. At the firing time T, the total input current is approximately equal to $J^\star$

$$J^\star \approx J(T) = I - I_{\mathrm{th}} - \sum_{i=1}^{k} g\mathrm{e}^{-(T-t_i^f)/\tau}(V_{\mathrm{th}} - E_{\mathrm{GABA}}) \tag{4}$$

and thus, the firing time of a neuron receiving a burst of k IPSCs is

$$T \approx \tau \ln g - \tau \ln(I - I_{\mathrm{th}} - J^\star) + \tau \ln(V_{\mathrm{th}} - E_{\mathrm{GABA}}) + \tau \ln \sum_{i=1}^{k} \mathrm{e}^{t_i^f/\tau}. \tag{5}$$

Let us now consider variable inhibition, i.e. the number k of received IPSCs is a random variable with mean $\langle k \rangle$ and variance σ_k^2, and the IPSC times t_i^f are drawn randomly from an unknown probability density function with variance σ_t^2. The only random variable in Eq. (5) is thus

$$X = \tau \ln \sum_{i=1}^{k} \mathrm{e}^{t_i^f/\tau}.$$

Furthermore, we have $\sigma_T^2 = \sigma_X^2$. An approximation for σ_T^2 can be found by considering the fact that the variance of a sum of a random number k of independent random variables, each with variance σ^2, is $\langle k \rangle \sigma^2 + \langle k \rangle^2 \sigma_k^2$, and that the variance of a function $y = g(x)$ of a random variable x approximately depends on the mean η_x and variance σ_x^2 of x: $\sigma_y^2 \approx |\mathrm{d}g/\mathrm{d}x|_{x=\eta}^2 \sigma_x^2$ (Eq. (5.56) in [17]). Using these formulae, we found

$$\sigma_T^2 \approx \frac{1}{\langle k \rangle}\left(\sigma_t^2 + \tau^2 \frac{\sigma_k^2}{\langle k \rangle}\right). \tag{6}$$

Note that Eq. (6) becomes identical to Eq. (4.20) in [2] when the inhibition is precise ($\sigma_t^2 = 0$). However, Eq. (6) is

more general than the one in [2] because it takes into account the fact that the IPSCs can occur at different times.

4. Numerical results

In order to check the validity of the approximation given by Eq. (6), we performed repeated simulations of the QIF neuron (Eq. (1), $I_{\text{noise}}(t) = 0$) receiving a random burst of k asynchronous synaptic events (Eq. (2)). The number k of unitary IPSCs is drawn randomly from a gaussian density with mean $\langle k \rangle = 100$ and standard deviation σ_k varying from 0 to 9. Unitary IPSCs are generated at random times (inhibitory jitter σ_t taken from 0 to 9 ms). In order to consider the effect of fast $GABA_A$ and slow $GABA_B$ inhibition, $\tau_{\text{fast}} = 6$ ms or $\tau_{\text{slow}} = 100$ ms have been used as synaptic decay time constant in Eq. (2).

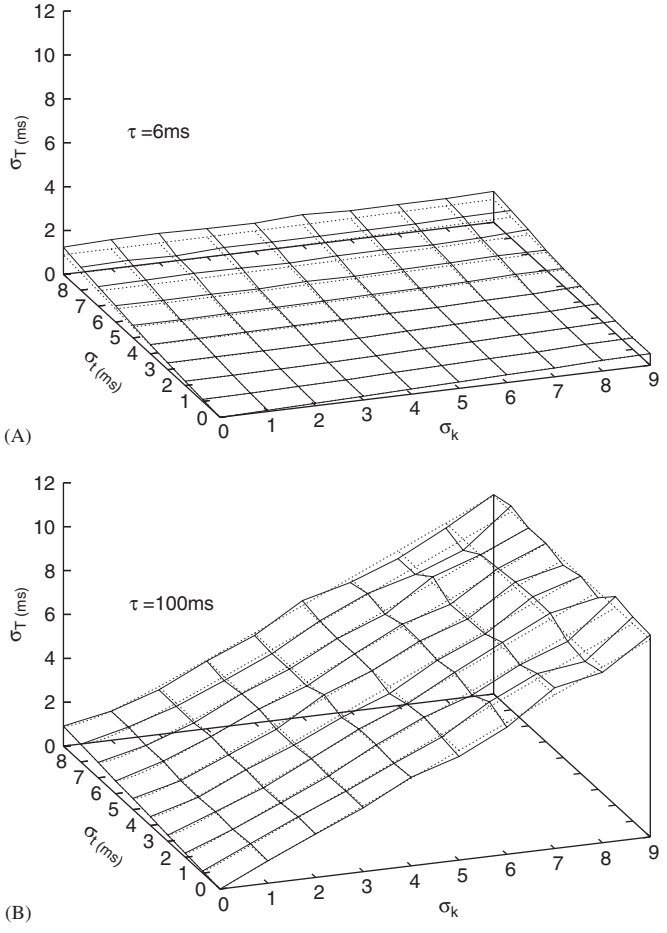

Fig. 4. Spike time jitter σ_T as a function of the variability of the received inhibition (σ_t, σ_k). The dashed curve represents theoretical σ_T values given by Eq. (6). The plain curve represents experimental σ_T values obtained from simulations of the QIF neuron. In Eq. (1), $I_{\text{noise}}(t) = 0$, $I = 0.13$ nA and I_{GABA} was obtained from a burst of k stochastic asynchronous synaptic events (Eq. (2)) with synaptic current decay of 6 ms (A) and 100 ms (B). The number k of unitary IPSCs is drawn randomly from a gaussian density with mean $\langle k \rangle = 100$ and standard deviation σ_k varying from 0 to 9. Unitary IPSCs are generated at random times (inhibitory jitter σ_t taken from 0 to 9 ms).

Fig. 4 compares the theoretical spike time jitter σ_T given by Eq. (6) to the one obtained from simulations. In Fig 4A, when fast inhibition is precise (small σ_t) and balanced ($k \approx \langle k \rangle$, small σ_k), we see a perfect match between theoretical and experimental σ_T values. For σ_t larger than 4 ms, σ_T values given by Eq. (6) are, however, underestimated. Moreover, the discrepancy between theoretical and experimental σ_T values increases with the inhibitory jitter σ_t. This is due to the approximations made for deriving Eq. (6). In particular, the approximation of the variance of a function (Eq. (5.56) in [17]) is only valid when the variance is small. From Eq. (6), we see that the inhibitory jitter contributes negatively to the spike timing precision through the ratio $\sigma_t^2/\langle k \rangle$. Because the mean number of IPSCs was large in our simulations, we obtained $\sigma_T \ll \sigma_t$ in case of fast inhibition (see Fig. 4A). From Fig. 4B, we see that slow inhibition is not robust to a variability on the number k of received IPSCs. The spike time jitter σ_T increases much faster in the σ_k direction in Fig 4B when $\tau_{\text{slow}} = 100$ ms than in Fig 4A when $\tau_{\text{fast}} = 6$ ms. When $\sigma_t = 0$, Eq. (6) predicts that σ_T will be $\tau_{\text{slow}}/\tau_{\text{fast}} \approx 17$ times higher for slow inhibition than for fast inhibition.

So far, we just considered a single burst of inhibition with $\langle k \rangle$ fairly large. What happens to the spike time jitter when $\langle k \rangle$ is smaller and the inhibition phasic? To address this question, we performed simulations of a QIF neuron receiving consecutive bursts of stochastic asynchronous synaptic events. Fig. 5 shows the temporal evolution of σ_T

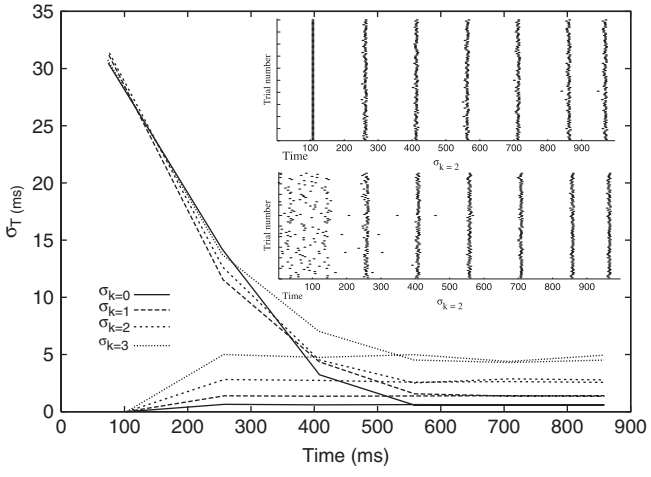

Fig. 5. With phasic fast GABAergic inhibition, the temporal evolution of the spike time jitter σ_T reaches a stable state. The QIF neuron (Eq. (1), $I_{\text{noise}}(t) = 0$) receives consecutive bursts of stochastic asynchronous synaptic events ($\langle k \rangle = 10$ IPSCs, $\sigma_t = 2$ ms, σ_k varying from 0 to 3 IPSCs, period of inhibitory bursts = 150 ms). Two extreme initial conditions are considered, one for which $V(t = 0)$ was similar in all trials and another for which $V(t = 0)$ was randomly chosen. They, respectively, lead to $\sigma_T = 0$ ms and $\sigma_T \approx 30$ ms at time $t = 100$ ms. Despite different initial conditions, σ_T converges to a stable state which depends on the value of σ_k. Two spike rasters, obtained from repeated trials with $I = 0.125$ nA, are indicated for the two initial conditions.

after consecutive bursts of inhibition with $\tau = 6$ ms. We see that σ_T reaches a stable state that does not depend on initial conditions but does depend on the value of σ_k.

5. Discussion

We have considered the spike timing precision of a neuron receiving GABAergic inhibition whose number and timing of inhibitory synaptic events is variable across repeated trials. How does this variability affect the spike timing precision in principal neurons? We have derived an approximate analytical expression for the spike output jitter (Eq. (6)). The variability of the received inhibition is characterized by the inhibitory jitter σ_t^2 and the variance σ_k^2 in the number k of inhibitory events. The inhibition is said to be balanced when σ_k^2 is small so that k across trials is approximately equal to the mean inhibition $\langle k \rangle$. The inhibition is said to be precise when σ_t^2 is small so that the inhibitory events occur approximately at the same time.

From Eq. (6), we see that the contribution of σ_t^2 and σ_k^2 to the spike output jitter σ_T^2 is divided by the mean inhibition $\langle k \rangle$ (large $\langle k \rangle$ implies small σ_T^2). In neural structures with a large number of inhibitory cells, $\langle k \rangle$ is expected to be large, and thus there is less requirement to have precise and balanced inhibition. In contrast, precise spike timing in neural structures where $\langle k \rangle$ is small requires precise and balanced inhibition. This prediction is in line with previous modeling work [15] and experimental data from the insect antennal lobe. The antennal lobe has a small number of inhibitory cells (e.g. 300 for the locust) and the inhibition has been shown to be very precise ($\sigma_t \approx 3.8$ ms, see [11]).

From Eq. (6), we see that the contribution of σ_k^2 to the spike output jitter σ_T^2 is multiplied by the decay time constant of the inhibitory synapse. As shown in Fig. 4, slow inhibition is not robust to a variability on the number k of received IPSCs, in contrast to fast inhibition. This result is in agreement with experimental data from the insect antennal lobe showing that synchronization and precise spike timing of principal cells decreases (resp. increases) when fast $GABA_A$ (resp. slow $GABA_B$) inhibition is pharmacologically blocked, see [21,24].

The role of phasic fast $GABA_A$ and slow $GABA_B$ inhibition is interesting to pursue as extension to this work. As seen in Fig. 5, the firing times of a neuron receiving consecutive bursts of fast inhibition become more and more precise over time. On the contrary, the spike time jitter of a residual neuron that does not receive inhibition or receive slow inhibition increases over time so that only its firing rate can reliably encode information (see Fig. 1). This suggests that complementary pieces of information may be conveyed in the precise timing of neurons receiving fast inhibition and in the firing rate of residual neurons receiving slow inhibition. Phasic fast and slow inhibition could, therefore, multiplex information into separate channels, in agreement with recent experimental work [7].

References

[1] R. Balu, P. Larimer, B.W. Strowbridge, Phasic stimuli evoke precisely timed in intermittently discharging mitral cells, J. Neurophysiol. 92 (2004) 743–753.
[2] C. Börgers, N. Kopell, Synchronisation in network of excitatory and inhibitory neurons with sparse, random connectivity, Neural Comput. 15 (2003) 509–538.
[3] R. Brette, E. Guigon, Reliability of spike timing is a general property of spiking model neurons, Neural Comput. 15 (2002) 279–308.
[4] A.P. Davison, J. Feng, D. Brown, Dendrodendritic inhibition and simulated odor responses in a detailed olfactory bulb network model, J. Neurophysiol. 90 (2003) 1921–1935.
[6] B. Ermentrout, Type 1 membranes, phase resetting curves, and synchrony, Neural Comput. 8 (1996) 979–1001.
[7] R.W. Friedrich, C.J. Habermann, G. Laurent, Multiplexing using synchrony in the zebrafish olfactory bulb, Nature Neurosci. 7 (2004) 862–871.
[8] B. Gutkin, G.B. Ermentrout, M. Rudolph, Spike generating dynamics and the conditions for spike-time precision in cortical neurons, J. Comput. Neurosci. 15 (2003) 91–103.
[9] H. Kashiwadani, Y.F. Sasaki, N. Uchida, K. Mori, Synchronized oscillatory discharges of mitral/tufted cells with different molecular receptive ranges in the rabbit olfactory bulb, J. Neurophysiol. 82 (1999) 1786–1792.
[10] N. Kopell, B. Ermentrout, Chemical and electrical synapses perform complementary roles in synchronization of interneuronal networks, Proc. Natl. Acad. Sci. 101 (2004) 15482–15487.
[11] G. Laurent, H. Davidowitz, Encoding of olfactory information with oscillating neural assemblies, Science 265 (1994) 1872–1875.
[12] G. Lowe, Inhibition of backpropagating action potential in mitral cell secondary dendrites, J. Neurophysiol. 88 (2002) 64–85.
[13] Z. Mainen, T. Sejnowski, Reliability of spike timing in neocortical neurons, Science 268 (1995) 1503–1506.
[14] T.W. Margrie, A.T. Schaefer, Theta oscillation coupled spike latenies yield computational vigour in a mammalian sensory system, J. Physiol. 546 (2) (2003) 363–374.
[15] D. Martinez, Oscillatory synchronization requires precise and balanced feedback inhibition in a model of the insect antennal lobe, Neural Comput. 17 (2005) 2548–2570.
[16] Z. Nusser, Release-independent short-term facilitation on GABAergic synapses in the olfactory bulb, Neuropharmacology 43 (2002) 573–583.
[17] A. Papoulis, Probability, Random Variables, and Stochastic Processes, second ed., McGraw-Hill Book Co., New York, 1984.
[18] S. Sachse, C.G. Galizia, The coding of odour-intensity in the honeybee antennal lobe: local computation optimizes odour representation, Eur. J. Neurosci. 18 (2003) 2119–2132.
[19] N.E. Schoppa, C.M. Kinzie, Y. Sahara, T.P. Segerson, G.L. Westbrook, Dendrodendritic inhibition in the olfactory bulb is driven by NMDA receptors, J. Neurosci. 18 (1998) 6790–6802.
[20] G.Y. Shen, W.R. Chen, J. Mitdgaard, G.M. Shepherd, M.L. Hines, Computational analysis of action potential initiation in mitral cell soma and dendrites based on dual patch recordings, J. Neurophysiol. 82 (1999) 3006–3020.
[21] M. Stopfer, S. Bhagavan, B.H. Smith, G. Laurent, Impaired odor discrimination on desynchronisation of odor-encoding neural assemblies, Nature 390 (1997) 70–74.
[22] N. Urban, B. Sakmann, Reciprocal intraglomerular excitation and intra- and interglomerular lateral inhibition between mouse olfactory bulb mitral cells, J. Physiol. 542 (2) (2002) 355–367.
[23] R. VanRullen, R. Guyonneau, S.J. Thorpe, Spike times make sense, Trends Neurosci. 28 (2005) 1–4.

[24] R.I. Wilson, G. Laurent, Role of GABAergic inhibition in shaping odor-evoked spatiotemporal patterns in the drosophila antennal lobe, J. Neurosci. 25 (40) (2005) 9069–9079.

Maxime Ambard received a master degree in computer engineering from the EPF School in Paris in 2001 and a master degree in cognitive sciences from the University Lumières in Lyon, in 2003. He is a PhD student at LORIA, CORTEX group, in Nancy. His main research interest is in computational neuroscience.

Dominique Martinez received his PhD degree in electrical and electronic engineering from the University Paul Sabatier in Toulouse, France, in 1992. He was a post-doctoral fellow at MIT, Department of Brain and Cognitive Sciences, and Harvard, VLSI group, in Cambridge, MA, USA, in 1992 and 1994, respectively. From 1993 to 1999 he worked at LAAS-CNRS in Toulouse where his research interests were concerned with machine learning (artificial neural networks, support vector machines). In 2000, he joined LORIA in Nancy and his research interests currently focus on biologically-plausible spiking neural networks for sensory processing, with particular application to artificial olfaction (neuromorphic electronic noses).